Journal of Combinatorial Mathematics and Combinatorial Computing
www.combinatorialpress.com/jcmcc

Combinatorial Press

Design of Interactive Control System for Agricultural Machines Based on AR and Deep Reinforcement Learning

Xiuni Li[1, ✉]

[1] *Xi'an Kedagaoxin University, Xi'an, Shaanxi, 710000, China*

ABSTRACT

Intellectualization of agricultural machinery can effectively improve the efficiency and quality of operations, and has an important role in promoting agricultural development. Based on AR technology, this paper introduces the key technology to build the interactive control system of agricultural machinery, uses NURBS to realize virtual agricultural machinery modeling, uses VRML technology to design a prototype of the scene environment of interactive farmland virtual reality, and details the methods of virtual modeling, virtual roaming, interactive control and collision detection in the process of system development. A four-degree-of-freedom simulation test bed is established to realize the simulation of the tractor's attitude when walking in the field. The position information of the crop rows is extracted from the virtual scene, and the control signals are given according to this information to carry out the speed, direction and balance control of the traveling of the agricultural machine, so that the tractor travels along the crop rows. The maximum deviations of the roll angle, pitch angle and yaw angle are within 0.36°, and the maximum deviations of the elevation and traveling speed are 2.11 mm and 0.14 km/h. The simulation analysis and the physical test show the feasibility of the interactive control system of the farm machine.

Keywords: AR technology, 3D modeling, virtual scene, VRML, interaction control, agricultural machinery

1. Introduction

With the rapid development of artificial intelligence technology, deep learning has been widely used in various fields. Agriculture, as a basic industry of the national economy, faces problems such as labor shortage and low production efficiency [1-2]. The introduction of deep learning technology into the field of agricultural machinery automation control is of great significance for improving agricultural production efficiency and reducing labor intensity.

✉ Corresponding author.
E-mail address: HHxx201320@163.com (X. Li).
Received 05 June 2024; Revised 20 August 2024; Accepted 05 December 2024; Published Online 16 April 2025.
DOI: 10.61091/jcmcc127b-045

Under the traditional agricultural production mode, farmers must be physically present to operate and supervise the working status of agricultural equipment, which not only consumes a large amount of human resources and time costs, but also limits the actual operational efficiency [3-6]. In contrast, by introducing a deep learning-based interactive control system, staff can use personal computers or portable smart terminals to realize the operation and management of field machinery and equipment, such as sowing, irrigation, fertilization and harvesting, and a series of agricultural activities [7-9]. Especially when performing large-scale irrigation tasks, the system can accurately regulate the working status of irrigation facilities according to the real-time data provided by the humidity sensing device installed in the soil, ensuring that each piece of cultivated land can receive the right amount of water supply [10-14]. It effectively prevents problems caused by over- or under-irrigation, thus providing a more ideal growing environment for crops, promoting the growth of yield and quality at the same time, and greatly improving the comprehensive efficiency of the entire agricultural production process [15-17]. In addition, the interactive control system can also instantly provide information about the operating status of agricultural machinery, operational details and field environment, so that farm managers can evaluate the growth of crops in different areas and their yield changes, so as to adjust the farming strategy and input resources [18-21]. In conclusion, the interactive control system of agricultural machinery based on artificial intelligence technology not only reduces resource consumption and environmental pollution, but also enhances the effective utilization of agricultural production resources and promotes the development of agricultural activities in the direction of more refinement [22-25].

The study incorporates AR technology for the overall design of the interactive control system of agricultural machines. Based on the three-dimensional interaction technology, the three-dimensional model of the virtual farm machine is established by using the non-uniform rational B-spline method. On the basis of fitting the uneven road surface using the harmonic superposition method, a digital simulation method is used to obtain the unevenness of the farmland, VRML technology is used to complete the 3D terrain modeling, and detail level modeling technology is used to improve the system's operating speed and interactive performance. Subsequently, the interactive function design of the system is carried out, the roaming of the virtual scene is briefly discussed, two input devices, keyboard and joystick, are used to realize the interactive control, and the AABB enclosing box algorithm is used for collision detection. On this basis, the virtual experimental field required for the platform test is constructed, the control performance of the platform with four degrees of freedom is analyzed, and the simulation test of human-computer interaction is carried out to explore the coordinate transformation in the physical scene and virtual environment.

2. Interactive control system design for agricultural machinery

Agriculture is the foundation of the national economy, the development level of agricultural machinery reflects the degree of agricultural modernization of a country. Therefore, the realization of agricultural machinery intelligence and human-computer interaction can provide strong and favorable support for intelligent agriculture, reduce the operating difficulty of agricultural machinery, make the operation process more accurate and intelligent, and at the same time effectively improve the efficiency and quality of agricultural machinery operations. In this paper, AR technology is integrated with the modeling theory of the virtual scene, and the modeling of agricultural machinery can be completed using this technology, which mainly includes: the appearance, behavior and function of the machinery. As the technology uses computers, it can form an intuitive image of the three-dimensional virtual environment.

In addition, real-time interaction between humans and machinery can also be realized. The meaning of human-computer interaction is to realize human-computer dialogue through the use of effective ways, with the help of software packages such as C++, Vega prime and other software packages to sum up the system, and to complete the overall development through the computer's input and output devices. The design of AR based interactive control system for agricultural machines consists of four main parts.

2.1. Large-screen display system

The display system of the interactive control platform for agricultural machinery is shown in Figure 1. The display system mainly contains the following parts: industrial control machine, projector, columnar metal screen and fusion machine, etc. In order to buy the three questions of the three-dimensional display needs to use six projectors to assist. In addition to the use of these six projectors can also be realized by 120 degrees of metal projection hard screen, fusion machine with edge fusion and nonlinear geometry correction function so that the three passes through the projection system can achieve the purpose of seamless splicing.

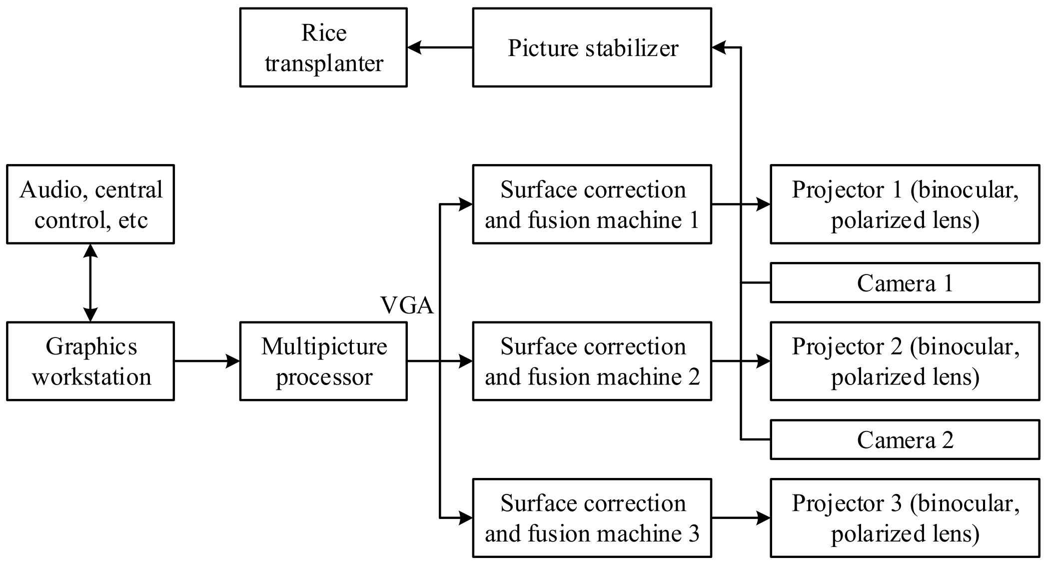

Fig. 1. The display system of the interactive control platform of the agricultural machine

2.2. Four-degree-of-freedom simulation platform

Four degrees of freedom refers to the four attitudes of vibration, steering, roll and pitch when the tractor operates in the field. The simulation platform of four degrees of freedom is composed of bracket, slewing frame, moving platform, vibration isolator, hydraulic cylinder and slewing motor, which contains the original parts such as accumulator, electro-hydraulic servo gate, hydraulic motor, hydraulic rotary joint, splitter and hydraulic source. The function of the diverter is to divide the 10MPa stabilized pressure oil provided by the hydraulic system into 3 ways through the action of the high pressure filter, and the pressure oil in the 3 ways respectively passes through 3 electro-hydraulic servo valves to go in and out from the cylinder constantly, and drive the cylinder to do lifting and lowering motion.

2.3. Three-dimensional modeling

The designers disassemble the solid of the agricultural machinery by taking accurate dimensional measurements of each of its parts and use the obtained data for 3D modeling of each part in Pro/E software. The constructed part model is converted and finally exported as a file with obj suffix. In Multigen Creator software, the model file with obj suffix is imported and converted into a part model in flt format. Finally, the flt format part model is assembled to obtain a complete 3D model of the agricultural machine.

2.4. Virtual test site

In the process of designing and planning the virtual test field of paddy field, in order to simplify the study, this paper chooses to regard the paddy field soil as a homogeneous and single state. Based on the study of the farmland conditions, crop growth conditions and digital maps of the cultivation area, a three-dimensional virtualization of the environment is made. The virtual test field includes the most basic paddy field, as well as the agricultural machinery, growing crops and field roads in it.

3. Virtual scenario construction

The virtual scene construction of the interactive control system of agricultural machinery based on AR technology includes scene modeling in two dimensions: virtual agricultural machinery and virtual farmland. The realization of the virtual scene is researched and developed in the program coding part using the high-level programming language Visual C++6.0 combined with the three-dimensional graphics development interface OpenGL.

3.1. Modeling of virtual agricultural machines

3.1.1. Three-dimensional modeling. The 3D model of the interactive control system of agricultural machinery has high requirements for realism and real-time, and it is necessary to reduce the complexity of the 3D model by means of re-modeling in order to facilitate the smooth rendering of the scene in the later stage. The virtual design of agricultural machinery is to design the actual parts, and the parts are composed of geometric shapes, and some methods are needed to accurately draw the geometry of the real object when building the model. The higher the complexity of the model, the longer the modeling time required and the more details, the slower the system runs and the lower the frame rate. In order to choose the appropriate modeling method for the parts, this paper mainly adopts the non-uniform rational B spline (NURBS) for 3D model modeling.NURBS establishes a 3D model by using curves and surfaces to describe the contours and shapes of the objects, and then draws a variety of complex parts by modifying the angle, number of points, and continuity of the curves, such as the body of the agricultural machinery, the engine, the gears, and pulley housings, etc. All can use this method for design and design. All of them can be designed and constructed by this method.

3.1.2. Three-dimensional graphic transformations. Three-dimensional graphic transformation is the transformation of geometric parameters to produce a new graphic, which is the core of the realization of virtual design. In the virtual design of agricultural machinery, graphics include two-dimensional and three-dimensional models, the attributes of object objects include spatial location, size and spatial angle, and when the attributes change, the object needs to be transformed by moving, scaling and converting. The 3D image transformation will use translation, scaling and rotation to convert the 3D graphics to other 3D graphics.

Suppose that $P=\begin{bmatrix} x & y & z & 1 \end{bmatrix}$ denotes a point in 3D space, $P=\begin{bmatrix} 4x' & y' & z' & 1 \end{bmatrix}$ denotes a new point after the transformation of the P-point, and the matrix of the transformation T is:

$$T=\begin{bmatrix} a & b & c & p \\ d & e & f & q \\ g & h & i & r \\ l & m & n & s \end{bmatrix} \tag{1}$$

Then, the expression for the graph transformation can be standardized as $P'=P\cdot T$, i.e:

$$\begin{bmatrix} x' & y' & z' & 1 \end{bmatrix} = \begin{bmatrix} x & y & z & 1 \end{bmatrix} \begin{bmatrix} a & b & c & p \\ d & e & f & q \\ g & h & i & r \\ l & m & n & s \end{bmatrix} \tag{2}$$

The 4×4 transformation matrix T of the 3D graph is partitioned into core functions, and the functions of each partition are:

1) The 3 × 3 matrix sub-block in the upper left corner can realize basic graphical transformations such as scale, rotation, symmetry and miscut, and its matrix expression is:

$$T = \begin{bmatrix} a & b & c & 0 \\ d & e & f & 0 \\ g & h & i & 0 \\ 0 & 0 & 0 & 1 \end{bmatrix} \tag{3}$$

2) The 1 × 3 matrix sub-block in the lower left corner is used to realize the translation transformation of the graph, and its matrix expression is:

$$T = \begin{bmatrix} 1 & 0 & 0 & 0 \\ 0 & 1 & 0 & 0 \\ 0 & 0 & 1 & 0 \\ l & m & n & 1 \end{bmatrix} \tag{4}$$

3) The 3 × 1 matrix sub-block in the upper right corner is used to realize the projection transformation of the graph, and its matrix expression is:

$$T = \begin{bmatrix} 1 & 0 & 0 & p \\ 0 & 1 & 0 & q \\ 0 & 0 & 1 & r \\ 0 & 0 & 0 & 1 \end{bmatrix} \tag{5}$$

4) The 1 × 1 matrix sub-block in the lower right corner is used to realize the scale transformation of the graph with the matrix expression:

$$T = \begin{bmatrix} 1 & 0 & 0 & 0 \\ 0 & 1 & 0 & 0 \\ 0 & 0 & 1 & 0 \\ 0 & 0 & 0 & s \end{bmatrix} \tag{6}$$

Three-dimensional image rotation change is a very important transformation, is an important method of agricultural machinery parts design, refers to the three-dimensional in space around the straight line rotation, generally along the X-axis, Y-axis or Z-axis axis of rotation, this paper around the Z-axis change of the three-dimensional image rotation design.

When point $P(x, y, z)$ is rotated counterclockwise around axis Z, the Z-axis of point P does not change, but only the X-axis and Y-axis change, and point M is rotated around axis Z as shown in Fig. 2. If the difference in the Z-axis is not taken into account, then a counterclockwise rotation from the P-point around the Z-axis to the P'-point is equivalent to a two-dimensional rotation from the M-point around the M'-point in the plane of the XOY-axis, that is, a two-dimensional rotation in the plane of the XOY-axis, with the coordinates of the $P'(x', y', z')$ -axis after the rotation:

$$\begin{cases} x' = x\cos\theta - y\sin\theta \\ y' = x\sin\theta + y\cos\theta \\ z' = z \end{cases} \tag{7}$$

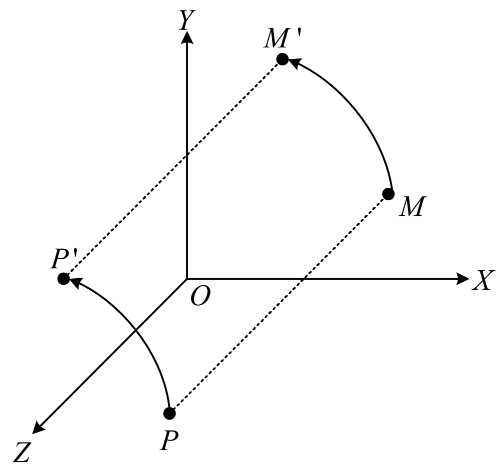

Fig. 2. Rotation diagram of Z-axis at M point

The rotation matrix T can be constructed as:

$$T = \begin{bmatrix} \cos\theta & \sin\theta & 0 & 0 \\ -\sin\theta & \cos\theta & 0 & 0 \\ 0 & 0 & 1 & 0 \\ 0 & 0 & 0 & 1 \end{bmatrix} \tag{8}$$

The expression of the rotation transformation matrix for the Z-axis is obtained as:

$$\begin{bmatrix} x' & y' & z' & 1 \end{bmatrix} = \begin{bmatrix} x & y & z & 1 \end{bmatrix} \begin{bmatrix} \cos\theta & \sin\theta & 0 & 0 \\ -\sin\theta & \cos\theta & 0 & 0 \\ 0 & 0 & 1 & 0 \\ 0 & 0 & 0 & 1 \end{bmatrix} \tag{9}$$

3.1.3. Three-dimensional agricultural machinery modeling process. In order to improve the accuracy of three-dimensional modeling of agricultural machinery parts, the parts modeling method of three-dimensional AR is adopted, and the parts modeling process is divided into the following steps:

1) For the AR immersive agricultural machinery parts design scene, point, line, surface and 2D image modeling technology is used to collect data on the 3D parts graphics and construct the 3D main framework of agricultural machinery parts.

2) Use image technology to perform three-dimensional cloud data acquisition of agricultural machinery parts, and fuse with the three-dimensional body framework in step 1) to realize coarse modeling of agricultural machinery parts.

3) Aiming at the local defects of the model in step 2), a 3D scanning system is used to carry out local scanning, and the theoretical method of virtual scene modeling is used to realize the fusion of points, lines and surfaces of different scales, so as to realize the fine modeling of agricultural machinery parts.

4) Rendering output three-dimensional parts, applied to agricultural machinery virtual reality and simulation.

3.2. Virtual Farmland Modeling

3.2.1. Farmland data acquisition. There are various kinds of 3D source data of farmland, mainly including topographic maps, thematic maps, satellite images, aerial images, existing data files, etc., as well as the corresponding massive attribute data, which contain layers or data types such as contour lines, elevation points, ditches, field roads, ridges, vegetation types, crops, etc. The source data of different formats are acquired in different ways, including full-field digital mapping, topographic map digitization, and digital photogrammetry. Different formats of source data are acquired in different ways, which are summarized in several ways, including full-field digital mapping, topographic map digitization, digital photogrammetry, and so on. In this paper, digital simulation is used to obtain farmland unevenness.

1) Harmonic superposition method to fit the uneven surface. The principle of harmonic superposition method to fit uneven road surface is to set the road surface elevation as a smooth, traversing the mean value of 0 Gaussian process, then can be simulated with different forms of triangular gradient. The following is described as an example of a sine wave. Random sine waves or other harmonic superpositions are used to discretize the numerical simulation of pavements using a model that approximates the target random process with a discrete spectrum. A random signal, such as a random wind pressure or road surface profile, can be decomposed into a series of sinusoids with different frequencies and amplitudes by a discrete Fourier analytic transform. The spectral density is then equal to the square of the amplitude of these sinusoids divided by the bandwidth.

The expression for fitting the power spectral density of the roadway surface unevenness displacement is given by the following equation:

$$G_d(n) = G_d(n_0)(\frac{n}{n_0})^{-w} n > 0 \tag{10}$$

where: n_0 - reference frequency, $n_0 = 0.1\text{m}^{-1}$, $G_d(n_0)$ - coefficient of unevenness of the road surface, m^2/m^{-1}, $G_d(n)$ - unevenness of the road surface, m^2/m^{-1}, w - frequency index, empirical value w = 2.

It is known that the spectral density of the pavement displacement within the spatial frequency $n_1 < n < n_2$ is $G_d(n)$. Using the spectral expansion property of the average power of a smooth stochastic process, the variance σ_z^2 of the pavement unevenness is:

$$\sigma_z^2 = \int_{n_1}^{n_2} G_d(n)dn \tag{11}$$

By dividing the interval (n_1, n_2) into n small intervals and taking the spectral density value $G_d(n_{mid-i})$ at the center frequency $n_{mid-i}(i = 1, 2, \cdots, n)$ of each small interval instead of $G_d(n)$ over the entire small interval, Eq. (11) is approximated after discretization:

$$\sigma_z^2 \approx \sum_{i=1}^{n} G_d(n_{mid-i}) \cdot \Delta n_i \tag{12}$$

Corresponding to each of the small intervals, now find the sine wave function with frequency $n_{mid-1}(i = 1, 2, \cdots, n)$ and its standard deviation is $\sqrt{G_d(n_{mnd-i}) \cdot \Delta n_i}$. Such a sine wave function can be:

$$\sqrt{2G_d(n_{mid-i}) \cdot \Delta n_i} \cdot \sin(2\pi n_{mid-i} x + \theta_i) \tag{13}$$

The sinusoidal wave functions corresponding to each of the subintervals are superimposed to obtain the frequency domain pavement random displacement input:

$$q(x)=\sum_{i=1}^{n}\sqrt{2G_d\left(n_{mid-i}\right)\cdot\Delta n_i}\cdot\sin\left(2\pi n_{mid-i}x+\theta_i\right) \tag{14}$$

where: θ - a uniformly distributed random number on $[0,2\pi]$, x - the X direction of the pavement in the frequency domain.

Since then, by discretizing the x value of the X direction of the pavement in the frequency domain, the value of the random pavement Y direction in the spatial frequency domain can be obtained.

2) Digital simulation method. RMS height is used to describe the variance of surface unevenness, also known as the standard deviation of surface unevenness, RMS height is the basic index of the measure of surface unevenness, and its calculation formula is:

$$\mathrm{h}_{\mathrm{rms}=}\sqrt{\frac{1}{n}\sum_{x=0}^{n}[Y(x)-\bar{Y}(x)]^2} \tag{15}$$

where, n - number of measured points, $Y(x)$ - height at surface x.

Simulation method:

Based on the road surface measurement interval of 1/m. Taking n=100, the inverse derivation of Eq. (15) was carried out to obtain the mean value of $Y(x)$. The data of n unevenness points were then obtained randomly based on the compromise method. The corresponding deviation σ_h was sought for the randomly generated data, and it was found that the error between the obtained results and the given σ_h in the table was less than 0.002, indicating that the unevenness data generated by the random simulation basically conformed to the actual situation.

3.2.2. 3D terrain modeling. The main content of a Virtual Modeling Language (VRML) file is the nesting of nodes and the definition and use of nodes, which form the entire 3D virtual world. The elevation raster nodes are used to create spatial surfaces, in the elevation raster nodes in the guide DEM (digital elevation model) data to generate three-dimensional terrain is the first choice of many researchers of three-dimensional terrain generation means, and are used in the VRML text editor to write text programs directly to achieve the way. In this paper, the VRML editing tool VRMLPAD is used to realize 3D terrain modeling.

3.2.3. Hierarchical model of terrain details. According to the structure type of the constructed terrain model, there are two main modeling methods: grid modeling and triangular grid modeling. Due to the complex structure of the triangular mesh terrain model, which is difficult to express in VRML, while the grid terrain model is easy to express with Elevation Grid nodes, so this topic chooses to build the grid terrain model. Before using VRML to display the 3D terrain, if the terrain data is not processed in some way, the large amount of data itself, coupled with the amount of computation of texture and lighting in the display process, makes the browser load is very heavy.

In order to solve these two problems need to use level-of-detail modeling technology (LOD), level-of-detail modeling refers to the objects in the scene in this paper refers to the digital elevation model, the use of different details of the description of the method of re-planning a set of models for drawing according to the object distance from the point of view of the choice of the use of the proximity.

The terrain detail level model is shown in Fig. 3, given the DME data, the elevation data at the nodes of the regular grid is known, for a row or a column of vertices A, B, C in the grid, any three vertices A, B, C, which form a triangle △AEB and △EBC with the point E, the angle formed by two triangular planes can be described by $a=\angle ACB$, the larger the a is, the more the two surfaces converge to be parallel, so it is possible to define a Simplified threshold parameter δ angle: when

$\delta > a$, vertex B can be simplified away and △AEC is used instead of △AEB and △BEC. When $a < \delta$, keep vertex B. In this way, it is possible to get to different levels of detail depending on the value of 6. When $\delta = n$, there is no simplification and the level of detail is the highest, and the level of detail gradually decreases as δ decreases.

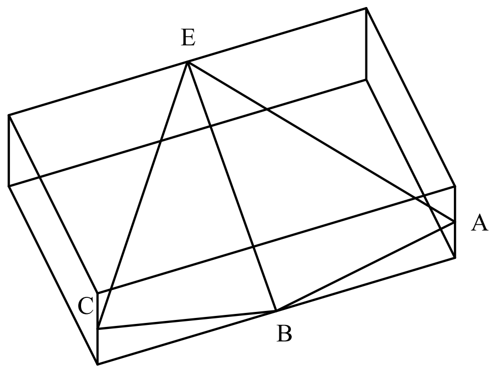

Fig. 3. Establishing the terrain detail level model

4. Interactive function realization

4.1. Virtual scene roaming

Virtual roaming is an important application of augmented reality technology, which realizes the virtualization and digitization of the three-dimensional landscape.OpenGL provides a gluLookAt (point of view, target point, point of view direction) function for observing the virtual world, whose main role is to change the observation point of the scene, which is equivalent to the human eye, and is also similar to the camera in the hands of the people.

The three parameters in the GluLookAt() function are three-dimensional coordinates, which are set as follows: the viewpoint is set to $E(ex, ey, ez)$, the viewpoint reference point is set to $C(cx, cy, cz)$, and the viewpoint direction is set to $U(ux, uy, uz)$. During the actual roaming process, considering the position of the observation point, the three parameters in the viewpoint direction $U(ux, uy, uz)$ are usually set to (0, 1, 0), and then a view matrix derived from the position and the upward direction of the viewpoint is generated by the OpenGL library function $gluLookAt(ex, ey, ez, cx, cy, cz, ux, uy, uz)$, whose viewing direction is determined by the line of sight connected to the reference point. A view matrix can be generated by OpenGL library function 4, which consists of the position of the viewpoint, the reference direction of the viewpoint, and a vector of upward directions, whose viewing direction is determined by the line of sight formed by the viewpoint and the reference point. The scene roaming control usually includes forward, backward, left/right rotation, upward and downward view operations, which are determined by controlling the line of sight from the viewpoint to the reference direction of the viewpoint. During the roaming process, user operations are continuously acquired, and then these operations are converted into specific variables, and then the corresponding changes are calculated through mathematical operations, and finally the gluLookAt() function is called to generate the scene model of the current viewpoint.

Let $A = \sqrt{(cx - ex)^2 + (cz - ez)^2}$, B be constants. When performing forward or backward operation, the viewpoint and reference point are calculated as follows:

$$ex = \frac{B * (cx - ex)}{A} + ex \tag{16}$$

$$ez = \frac{B * (cz - ez)}{A} + ez \tag{17}$$

$$cx = \frac{B*(cx - ex)}{A} + cx \tag{18}$$

$$cz = \frac{B*(cz - ez)}{A} + cz \tag{19}$$

Feedback on the different movement directions is provided by setting the constant B positive or negative, when B is positive, it means forward movement, and vice versa, backward movement.

When performing left-right rotation, the viewpoint and reference point are calculated by the formula:

$$cx = (cx - ex)\cos(A/360) + (cz - ez)\sin(A/360) + ex \tag{20}$$

$$cz = (cz - ez)\cos(A/360) - (cx - ex)\sin(A/360) + ez \tag{21}$$

4.2. Interactive control

In order to be able to interact with the farm machinery in the virtual scene, the keyboard and joystick are used to realize the interactive control, while its corresponding control commands will be sent to the controller of the execution end of the agricultural vehicle through the network.

4.2.1. Keyboard Interaction Control. You can define certain keys on the keyboard to correspond to some actions, and in the program design, by constantly capturing user key operations and converting them into corresponding control commands, you can finally realize the change of scene display.

4.2.2. Joystick Interaction Control. DirectInput is a set of APIs for mouse, keyboard, joystick, and force feedback devices. The key to interaction control is the combination of DirectInput data with the motion model of the agricultural machine. The main considerations in the design of the motion model of the agricultural machine are: start, stop, direction, speed, brake, and gear shift. According to the numerical changes of the above components to control the movement of the virtual farm machine, at the same time, these control signals will be sent to the field controller of the execution end of the agricultural vehicle through the network, and the field controller will analyze the control signals and then send the real-time control commands to the various control units of the vehicle, so as to realize the operation of the real vehicle.

4.3. Collision Detection

A fast and accurate collision detection algorithm can enhance the immersion of the virtual environment, while the complexity and real-time nature of the virtual environment itself put forward higher requirements for collision detection. Taking into account the computing speed, the accuracy of collision detection and the shape of the objects in the virtual scene, the AABB enclosing box algorithm is used for collision detection. At the beginning of detection, if no collision occurs at this time, the system responds to the user operation and updates the position of the moving object (virtual vehicle). If a collision is detected, the position of the moving object is adjusted accordingly to avoid collision.

The Axial Bracket Box (AABB) is a cubic box that wraps around the whole or a major part of a 3D object, and then calculates whether a collision occurs based on the distance and position of the box. The box of AABB is parallel to the OpenGL axes, and each face of the box is perpendicular to one axis, which can reduce the number of operations when transforming the box.

For a given object, the calculation of its AABB enclosing box is very simple, it is only necessary to obtain the maximum and minimum values in the direction of coordinate axis x, y, z according to the shape and state of the object at the time of construction or to determine the enclosing box by the center of gravity and corner points. Each way of definition is as follows:

1) Definition based on the maximum and minimum values in the x, y, z-direction. Assuming that the maximum and minimum values of the projections of the vertices of the elements on the x, y, z coordinate axes of the set of basic geometric elements of the enclosing object are $x_{max}, y_{max}, z_{max}$ and $x_{min}, y_{min}, z_{min}$, respectively, any point P within the enclosing box has:

$$P = \{(x, y, z) \mid x_{min} \le x \le x_{max}, y_{min} \le y \le y_{max}, z_{min} \le z \le z_{max}\} \tag{22}$$

2) According to the definition of the center of gravity of the enclosing box. Assuming $C(x_e, y_e, z_e)$ is the coordinate of the center of gravity of the enclosing box and D_x, D_y, D_z is the length of the enclosing box respectively, we have:

$$P = \{(x, y, z) \mid | x_c - x | \le D_x, | y_c - y | \le D_y, | z_c - z | \le D_z\} \tag{23}$$

3) Based on the definition of corner points of the enclosing box. Assuming $O(x_0, y_0, z_0)$ is the coordinate of a corner point of the enclosing box and D_x, D_y, D_z is the length of the enclosing box respectively, we have:

$$P = \{(x, y, z) \mid x_0 \le x \le x_0 + D_x, y_0 \le y \le y_0 + D_y, z_0 \le z \le z_0 + D_z\} \tag{24}$$

5. Experimental analysis of agricultural machinery interaction control

According to the above method, the virtual scene of farmland and the simulation of field working conditions are carried out, in which the simulation test bench has 4 degrees of freedom to realize the simulation of the attitude (including vibration, steering, cross roll and pitch) of the tractor when walking in the field.

5.1. Simulation test rigs

The virtual scene test bench of agricultural machinery mainly consists of a four-wheeled turntable, rice transplanter, virtual scene, computer, motion console, connecting device and sensing and testing equipment, etc. The rice transplanter automatically travels on the base of the parallel machine through the turntable.

The field condition simulator consists of a motion platform that can change the spatial position, a fixed base frame, and six supporting rods with the same structure and adjustable length connecting the small turntable and the base frame. The rods and the platform are connected by a Hooke hinge, and the support rods of the platform are driven by an electro-hydraulic servo system, thus realizing the change of the displacement of the rods.

The computer extracts information about the change of terrain, the direction of crop rows and possible obstacles within the virtual scene, and sends control signals to the field condition simulation platform to show the characteristics of the ground by controlling its height, roll angle, pitch angle and direction.

5.2. Platform performance testing and analysis

The test stand is capable of four degrees of freedom, including up and down vibration, horizontal roll, pitching and steering. Commissioning of the test stand and its control system.

5.2.1. Experiments on roll angle control. The cross roll angle requires a maximum adjustment angle of 10° and a control accuracy of ±1°. Run the control motor and increase the pressure to 10MPa for the hydraulic system. Run the upper computer control software to initialize the simulation platform. Install the laser range finder, electronic compass and other VG measuring instruments or devices on the motion platform, connect to the monitoring system computer through the serial port, and read the VG data installed on the platform in real time from the monitoring computer.

Control the hydraulic cylinder to realize the rolling of the platform. The desired deflection angle is given on the upper computer, and every increment or decrement of 1°, the reading of the cross roll angle on the monitoring computer is read, and the results of the debugging data of the cross roll angle are shown in Figure 4. The test is divided into two processes of left flip control and right flip return control, and the desired input of the traverse roll angle is very close to the actual angle of the traverse roll angle, and the error is kept within the range of -0.40°~0.41°.

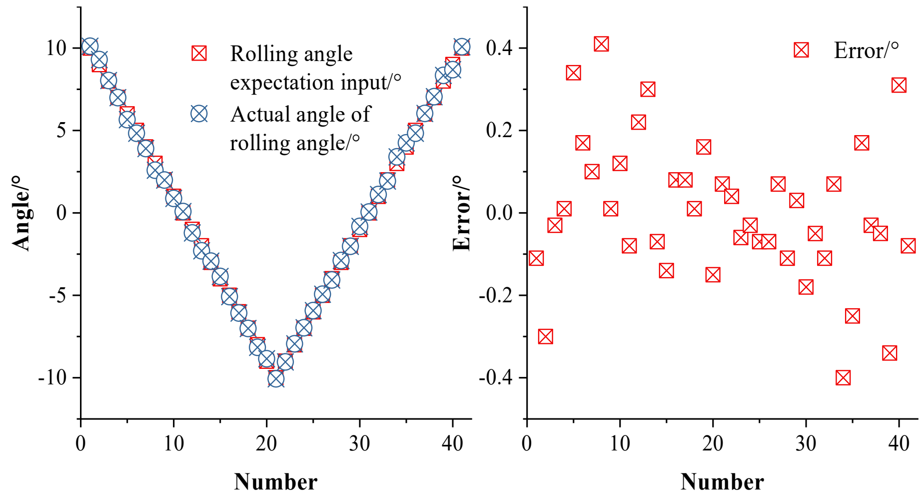

Fig. 4. Debugging data result for rolling angle

5.2.2. Pitch angle control experiment. Control the hydraulic cylinder to realize the pitch of the platform. The desired pitch angle is given on the upper computer, and the reading of the pitch angle on the monitoring computer is read every 1° increment or decrement, and the debugging data result of the pitch angle is shown in Fig. 5, and the error between the given pitch angle and the actual pitch angle is within 0.64°.

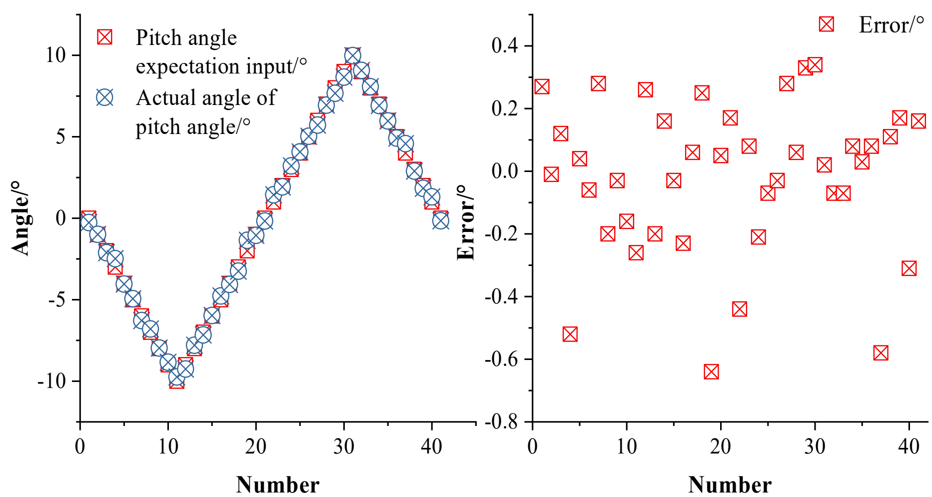

Fig. 5. Debugging data result for pitch angle

5.2.3. Rotation angle control experiment. First initialize the simulation simulation platform and make its rotation angle zero. According to the clockwise direction of rotation, such as rotation to the clockwise direction of the maximum angle that is 45 °, control the movement platform reverse movement, to reach the maximum angle of the reaction, that is, counterclockwise direction of the

-45 ° angle, and then let the rotating platform clockwise rotation, to re-return to the initial state position. Run to get the results of the angle input value and the actual angle when turning clockwise, Figure 6 shows the results of the debugging data of the rotation angle, the deviation of the theoretical rotation angle from the actual rotation angle is within the range of -0.4°~0.4°.

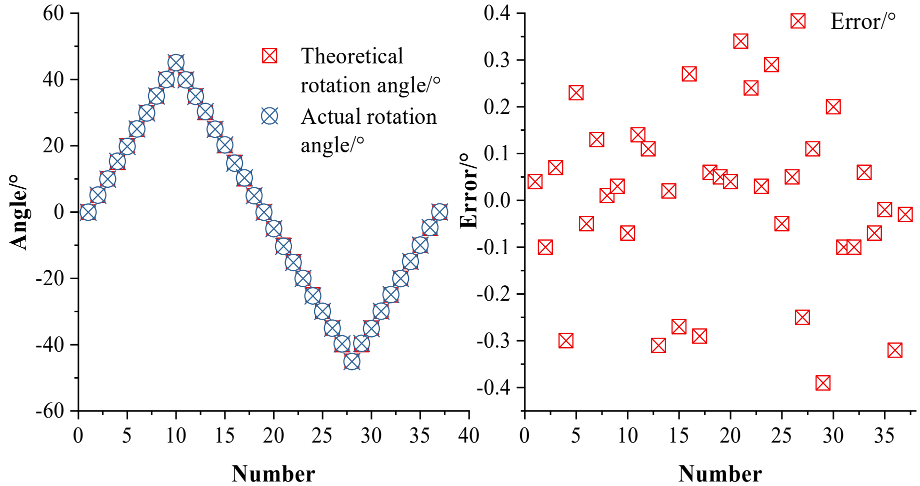

Fig. 6. Debugging data result for rotations angle

5.2.4. Altitude control experiments. To achieve height control, synchronized control of the three hydraulic cylinders is required. The operation control motor increases the pressure to 10 MPa to the hydraulic system. Continuously change the servo valve control signals of the three hydraulic cylinders, so that the simulation platform maintains the horizontal state while the height changes continuously. Read the signal of the laser distance measuring sensor installed on the motion platform, and after data processing, the data results of the height control are shown in Figure 7. It can be seen that the maximum error of the height control is 2.9mm.

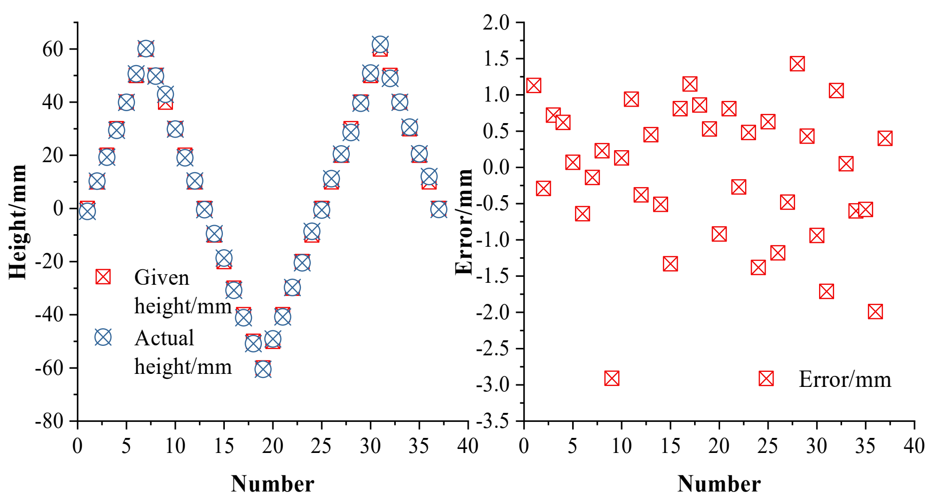

Fig. 7. Highly controlled data results

5.3. Human-computer interaction simulation test

Run the farmland virtual test scene software, generate terrain data, and call in the three-dimensional simulation model of agricultural machinery. Start the hydraulic control system to drive the four degrees of freedom simulation platform operation. Start the physical prototype model of agricultural machinery.

On the virtual test scene software, give the agricultural machinery three-dimensional model initial speed, so that it is traveling along the crop rows in the virtual scene. Calculate the traction force on the virtual prototype and terrain data, combined with the virtual prototype walking speed and six degrees of freedom data, through the embedded controller to drive the hydraulic cylinders and hydraulic motors to realize the control of the physical prototype.

Laser range sensors, gyroscopes and UGs are installed on the four-degree-of-freedom simulation platform to collect the attitude data of the simulation platform, and Hall sensors are installed on the wheels of the prototype to detect the rotation speed of the wheels. The system records the virtual scene terrain feature data and virtual prototype attitude information in real time, and the test data of virtual prototype and physical prototype control are shown in Table 1 and Table 2, respectively. The maximum deviation of the roll angle is 0.34°, the maximum deviation of the pitch angle is 0.25°, the maximum deviation of the yaw angle is 0.36°, the maximum deviation of the elevation is 2.11 mm, and the maximum deviation of the traveling speed is 0.14 km/h. The attitude of the motion platform and the traveling speed of the physical prototype have a better consistency with the attitude of the virtual scene and the virtual prototype.

Table 1. Parameter of virtual machine

Time/s	The location of the virtual prototype				Virtual scene speed/km*h-1
	Rolling Angle/°	Pitch Angle/°	Yaw Angle/°	Altitude/mm	
1	3.24	0.41	-4.76	22.82	6.28
2	3.03	0.84	-4.51	24.15	6.37
3	2.71	0.95	-3.49	26.65	6.49
4	2.26	1.05	-2.36	31.88	6.31
5	1.42	1.13	-1.22	35.68	6.24
6	1.29	1.47	-0.89	39.68	6.43
7	0.43	1.81	-0.43	42.36	7.14
8	0.81	2.26	0.71	40.12	7.19
9	-0.37	2.67	1.33	38.1	7.23
10	-1.35	2.43	1.86	36.37	6.94
11	-1.52	2.15	2.21	32.12	6.76
12	-2.18	2.09	2.84	29.06	6.54
13	-2.57	1.89	3.13	27.21	6.66
14	-3.07	1.62	3.46	24.08	6.72
15	-3.25	1.48	3.52	22.97	6.86

Table 2. Parameter of entity machine

Time/s	The posture of the four-self simulation platform				Actual walking speed/km*h-1
	Rolling Angle/°	Pitch Angle/°	Yaw Angle/°	Altitude/mm	
1	3.49	0.49	-4.96	23.92	6.39
2	3.15	0.78	-4.76	23.04	6.26
3	3.03	0.86	-3.82	27.71	6.67
4	2.2	1.06	-2.64	33.99	6.21
5	1.36	1.22	-0.93	34.75	6.28
6	1.54	1.48	-1.25	41.18	6.52
7	0.12	1.56	-0.35	43.48	7.17
8	0.84	2.12	0.61	41.11	7.13
9	-0.03	2.77	1.17	39.04	7.16
10	-1.32	2.39	1.77	34.43	7.32
11	-1.29	1.92	2.2	31.01	6.74
12	-2.03	2.09	2.83	30.05	6.68
13	-2.59	1.76	3.10	26.29	6.69
14	-3.14	1.46	3.58	25.93	6.84

15	-3.28	1.58	3.49	24.17	6.75

6. Conclusion

This paper mainly designs the interaction control system of agricultural machinery, combines AR technology to construct virtual farm machinery scene and virtual farmland scene, designs the interaction control method of the system, builds out the simulation test platform, explores its performance through experiments, and analyzes the interaction control simulation experiments. The main research results are as follows:

1) From the four dimensions of traverse angle, pitch angle, rotation angle and height control, experiments are conducted on the simulated test platform, and the error results of the experimental expected values and the actual output are small, which are controlled within 0.41°, 0.64°, 0.40° and 2.9 mm, respectively, which verifies the good performance of the test platform and its control system.

2) The maximum deviations of traverse angle, pitch angle, yaw angle, elevation and travel speed are 0.34°, 0.25°, 0.36°, 2.11 mm and 0.14 km/h, respectively, and there is a better consistency between the physical prototype and the virtual prototype, which realizes the synergistic control of the physical prototype of the agricultural machinery, the three-dimensional simulation model of the agricultural machinery, and the virtual experimental field.

3) Based on AR and deep reinforcement learning technology, this paper researches the interaction control system of agricultural machinery, which can simulate the movements of four degrees of freedom, such as vibration, steering, tilting and pitching, etc., when the agricultural machinery works in the field. Due to the limitation of time and research conditions, individual experiments are subject to further research. In terms of human-computer interaction between the field working condition simulation platform and the scene displayed on the big screen, it is necessary to carry out research on the co-simulation of virtual man, virtual prototype and virtual environment.

References

[1] Yuanling, H. E., Zebing, X. I. N. G., Huaming, H. O. U., & Xiaodong, W. U. (2019). Development Status and Prospect of Intelligent Agricultural Machinery Equipment. *Journal of Agricultural Science & Technology* (1008-0864), 21(6).

[2] Aby, G. R., & Issa, S. F. (2023). Safety of automated agricultural machineries: a systematic literature review. *Safety*, 9(1), 13.

[3] LIU, W. (2024). Interactive Display Design of Agricultural Machinery Based on Virtual Reality Technology. *Journal of Agricultural Mechanization Research*, 46(12), 199-203.

[4] Che, Y., Zheng, G., Li, Y., Hui, X., & Li, Y. (2024). Unmanned Agricultural Machine Operation System in Farmland Based on Improved Fuzzy Adaptive Priority-Driven Control Algorithm. *Electronics*, 13(20), 4141.

[5] Zhao, X., Du, Y., Mao, E., Zhu, Z., & Song, Z. (2022). Agricultural tractor dynamics simulation research based on a driving simulator with real-time human-machine interaction. *Computers and Electronics in Agriculture*, 203, 107443.

[6] Li, C. E., Tang, Y., Zou, X., Zhang, P., Lin, J., Lian, G., & Pan, Y. (2022). A novel agricultural machinery intelligent design system based on integrating image processing and knowledge reasoning. *Applied Sciences*, 12(15), 7900.

[7] Zhang, P., Lin, J., He, J., Rong, X., Li, C., & Zeng, Z. (2021). Agricultural machinery virtual assembly system using dynamic gesture recognitive interaction based on a CNN and LSTM network. *Mathematical Problems in Engineering*, 2021(1), 5256940.

[8] Zhang, F., Zhang, W., Luo, X., Zhang, Z., Lu, Y., & Wang, B. (2022). Developing an IoT-enabled cloud management platform for agricultural machinery equipped with automatic navigation systems. *Agriculture*, 12(2), 310.

[9] Yin, X., Wang, Y., Chen, Y., Jin, C., & Du, J. (2020). Development of autonomous navigation controller for agricultural vehicles. *International journal of agricultural and biological engineering*, 13(4), 70-76.

[10] Lorenz, S. (2023). Design of a teleoperation user interface for shared control of highly automated agricultural machiness. *Proceedings of the Design Society*, 3, 1277-1286.

[11] Panfilov, I., & Mann, D. D. (2018). The Importance of Real-Time Visual Information for the Remote Supervision of an Autonomous Agricultural Machine. *Canadian Biosystem Engineering Journal*, 60.

[12] Wang, H., Ma, Z., Ren, Y., Du, S., Lu, H., Shang, Y., ... & Fu, W. (2024). Interactive image segmentation based field boundary perception method and software for autonomous agricultural machinery path planning. *Computers and Electronics in Agriculture*, 217, 108568.

[13] Zhao, Y., Qi, H., Xu, W., & Li, J. (2018, October). Research on master-slave controlling remote operation of live working robots in agricultural distribution network. *In 2018 IEEE 3rd Advanced Information Technology, Electronic and Automation Control Conference* (IAEAC) (pp. 1401-1405). IEEE.

[14] Badgujar, C., Das, S., Figueroa, D. M., & Flippo, D. (2023). Application of computational intelligence methods in agricultural soil–machine interaction: A review. *Agriculture*, 13(2), 357.

[15] Zhu, L., & Fan, R. (2020, April). Convenience of voice interaction design in the 5g era to adapt to agricultural machinery. *In 2020 Asia-Pacific Conference on Image Processing, Electronics and Computers* (IPEC) (pp. 208-212). IEEE.

[16] Zhao, J., & Mao, E. (2022). Emerging automated technologies on tractors. *In Sensing, data managing, and control technologies for agricultural systems* (pp. 203-222). Cham: Springer International Publishing.

[17] Ma, L., Ikbal, M., & Cengiz, K. (2021). Realization of agricultural machinery equipment management information system based on network. *International Journal of Agricultural and Environmental Information Systems* (IJAEIS), 12(3), 13-25.

[18] Vasconez, J. P., Kantor, G. A., & Cheein, F. A. A. (2019). Human–robot interaction in agriculture: A survey and current challenges. *Biosystems engineering*, 179, 35-48.

[19] Zhang, Z., Liu, H., Meng, Z., & Chen, J. (2019). Deep learning-based automatic recognition network of agricultural machinery images. *Computers and Electronics in Agriculture*, 166, 104978.

[20] Padhiary, M. (2025). The Convergence of Deep Learning, IoT, Sensors, and Farm Machinery in Agriculture. *In Designing Sustainable Internet of Things Solutions for Smart Industries* (pp. 109-142). IGI Global.

[21] Hassan, M., Kowalska, A., & Ashraf, H. (2023). Advances in deep learning algorithms for agricultural monitoring and management. *Applied Research in Artificial Intelligence and Cloud Computing*, 6(1), 68-88.

[22] Thomas, G., Balocco, S., Mann, D., Simundsson, A., & Khorasani, N. (2021). Intelligent agricultural machinery using deep learning. *IEEE Instrumentation & Measurement Magazine*, 24(2), 93-100.

[23] Hengyi, Z., & Ahamed, T. (2024). Driver Safety System for Agricultural Machinery Operations Using Deep Learning Algorithm. *In IoT and AI in Agriculture: Smart Automation Systems for increasing Agricultural Productivity to Achieve SDGs and Society 5.0* (pp. 99-122). Singapore: Springer Nature Singapore.

[24] Zhang, Q., Liu, Y., Gong, C., Chen, Y., & Yu, H. (2020). Applications of deep learning for dense scenes analysis in agriculture: A review. *Sensors*, 20(5), 1520.

[25] Patel, G. S., Rai, A., Das, N. N., & Singh, R. P. (Eds.). (2021). Smart agriculture: emerging pedagogies of deep learning, machine learning and internet of things. *CRC Press*.